Electrical Characterization and Modeling of High Frequency Arcs for Higher Voltage Aerospace Systems

DOI:
10.1109/TTE.2023.3244776

Document Version
Accepted author manuscript

Published in:
IEEE Transactions on Transportation Electrification

TTE-Reg-2022-11-1840

Electrical Characterization and Modeling of High Frequency Arcs for Higher Voltage Aerospace Systems

Abir Alabani, *Student Member, IEEE*, Prem Ranjan, *Member, IEEE*, Jun Jiang, *Senior Member, IEEE*, Lujia Chen, *Member, IEEE*, Ian Cotton, *Senior Member, IEEE*, Vidyadhar Peesapati, *Member, IEEE*

***Abstract*—Arcing in future high-voltage aerospace systems could occur more frequently and cause irreversible damage to electrical components, system structure and increase the risk of fire. While arcs seen in low-voltage aerospace systems tend to be long-duration and low-energy events, higher power but short-duration arcs may occur in high-voltage aerospace systems if they are readily detectable by system protection. This paper investigates the characteristics of high current arc faults generated at the AC frequencies expected in future rotating machines used for higher voltage aerospace systems. As such, arcs with a peak current up to 4.6 kA are generated at frequencies in the range of 0.5-2 kHz using an underdamped RLC circuit, under pressures of 0.2-1 bar absolute. High frequency arcs exhibit a similar characteristic to lower frequency arcs. A reduction in pressure results in lower arc voltage and arc power. Arcing tests at atmospheric pressure may therefore represent a worst-case scenario and the development of a low-pressure test environment may not be necessary. A black box model is developed to provide good agreement with experimental arc voltage waveforms for different parameters investigated in this study. This is a generalized modeling approach to estimate high-frequency high-voltage arcing characteristics without recourse to experiment.**

***Index Terms*— Arc discharges, arc flash, arc model, high frequency, high-voltage techniques, aircrafts and decarbonization.**

I. INTRODUCTION

DECARBONISATION is considered an essential pillar in creating a more sustainable environment as part of the European Green Deal [1]. Direct emissions from the aviation sector are responsible for approximately 2% of the global greenhouse gas emissions [2]. There is an urgent need to develop aircraft with electrical systems operating at higher voltages to enable the power levels required in all-electric or hybrid electric propulsion systems [3]. With the need for future aerospace electrical systems to be power-dense, there is a continued effort to increase the operating voltage of these systems. According to [4], future hybrid aircrafts are expected to see an increase in the power demand up to 5 MW, which raises the operating system voltage to 1-3 kV. Self-contained networks, where generation, distribution and transmission are achieved on-board, give AC power generation an advantage with variable frequency systems going up to 2 kHz to reduce weight/size of electrical machines [5]. Previous work has shown that while the introduction of higher voltage power systems in aircraft enhances their efficiency, this has also introduced an increased probability of high-voltage faults that could lead to arcs and major failures in aircraft electrical systems [3]. As with any electrical system, there is an expectation that faults will occasionally take place in insulation systems and arcs will develop as a result. Managing arcs that arise from electrical faults in aerospace electrical systems have previously been challenging given the lower operating voltage of the electrical system and low levels of fault current [5]. This has resulted in aerospace cabling systems being designed to withstand the effects of sustained arcing due to wiring faults.

The majority of the arcing faults observed in aircraft have been attributed to being caused by insulation degradation and the subsequent short-circuit (accounted for more than half of the total failures in the period of 1980-1999) [3], [6]. Given the voltage of these systems has been below Paschen's minimum, arcs are ignited when either an electrode gap is short-circuited by a physical connection (e.g., a wire rubbing against a metallic flange) or due to a conductive material travelling into the air gap between two conductors (e.g., contaminated water dripping onto cracked insulation). As arcs propagate on the cable surfaces or to adjacent circuits and conductors, they can cause severe damage to the component or the wider electrical system [7].

Previous research focused on understanding the characteristics of arcs in aircraft for 28 VDC and 115 VAC systems (as used on platforms such as the Boeing 737 / Airbus

Manuscript received 21 June 2022, revised 21 November, and accepted 29 January 2023. This work was funded by the EU Horizon 2020 Research and Innovation Framework Programme for the Clean Sky 2 Joint Undertaking under grant agreement number 864717. For the purpose of open access, the author has applied a CC BY public copyright license to any Author Accepted Manuscript version arising from this submission *(Corresponding authors: Lujia Chen and Ian Cotton).* Abir Alabani and Prem Ranjan are co-first authors.

Abir Alabani, Prem Ranjan, Lujia Chen, Ian Cotton and Vidyadhar Peesapati are with the Department of Electrical and Electronic Engineering, The University of Manchester, Manchester, M13 9PL, UK (e-mail: abir.alabani@postgrad.manchester.ac.uk; prem.ranjan@manchester.ac.uk; lujia.chen@manchester.ac.uk;ian.cotton@manchester.ac.uk; v.peesapati@manchester.ac.uk). Jun Jiang is with the Department of Electrical and Electronic Engineering, Nanjing University of Aeronautics and Astronautics, Nanjing 211106, Jiangsu Province, China (e-mail: jiangjun0628@163.com).

A320). More recent work has extended this to consider the incremental voltage steps of 230 VAC / 540 VDC seen on systems such as the Boeing 787 / Airbus A350. Significant work was carried out to investigate the nature of DC arcs in an aerospace environment at the time 540 V DC systems were introduced. In these DC systems there is a specific challenge associated with current interruption due to the absence of current zero. The results in [8]–[11] provide information on what is expected of an AC using RMS values (e.g., arc voltage reducing at low pressure) but there is no prior work in the public domain that explores high frequency AC arcs in an aerospace environment. In [8], DC arcs in the range of 7 to 300 A were shown to have a lower arc voltage as pressure reduces. The dissipated mean arc energy increased for higher currents and lower pressures which is not the result of a higher arc voltage per unit length but due to the arc elongation. Investigations in [9] and [10] for DC arcs at 540 V and a current range of 10 to 100 A, showed a non-linear increase of arc dissipated energy with system voltage and an unclear variation of energy as a function of pressure.

For previous AC arcs, investigations were mostly conducted on arc currents ranging from 10 to 350 A_{rms} with system voltages under 500 V and frequencies up to 850 Hz [7], [12]–[16]. An increase in the operating frequency of AC arcs, from 360 to 850 Hz in [12], [13] leads to a reduction in the current interruption capability and shortening of the "flat-shoulder" occurring at the current zero crossing. At a frequency of 850 Hz, it was found that the rate of change of current, *di/dt* is higher than at 360 Hz which weakens the insulating gas recovery process [13] and escalates the deterioration of cable insulation [17].

The continuous development of electric power systems on aircrafts and the potential increase in the system voltage to 3 kV, as used the in E-fan X demonstrator [18], [19], is seen as a technical challenge on the safe operation of aircrafts especially with other evolutionary changes demanding optimized designs, improved efficiency, and higher power density. This is amplified by the presence of demanding mechanical and environmental conditions. On a power system level, this imposes a threat on the insulation systems and fault management. At lower voltages, the arc voltage is more likely to be significant in comparison to the system voltage and as a result will lower the current flowing through a fault. In higher voltage systems where arc voltages become proportionally smaller to the system voltage, the fault current is increasingly determined by the system impedance and may increase significantly. This paper presents experimental work carried out to examine the characteristics of AC arcs under pressures of 0.2 to 1 bar, frequencies of 0.5 to 2 kHz and a peak arc current up to 4.6 kA. The experimental investigations are to: (i) inform the development of a high frequency aerospace arc model that can accurately evaluate different arc parameters without having to conduct a large volume of experimental work, and (ii) identify test techniques that could be used to qualify future higher voltage aerospace electrical systems. Arc energy was calculated based on the experimental data to examine the effects of various measurands including the arc length. A modified black box model has been developed that can provide good agreement with experimentally obtained arc parameters. The developed model in this work has wider implications in terms of assessing the impact of high frequency arcs on higher voltage aerospace applications.

II. Experimental Setup and Data Processing

A. High Current Test Circuit

As shown in Fig. 1, the circuit consists of a capacitor bank (each capacitor being 1,500 µF) charged with a DC power supply (125 kV, 30 mA, Glassman) through a 10 kΩ charging resistor, R_C. Resistors, R_{eq} of 100 kΩ are connected across each capacitor, C to ensure equal voltage distribution during charging and to act as bleed resistors after testing. A safety earth switch (monostable pneumatic control) is connected in series to a 1 kΩ resistor, R_{dump} and connected in parallel to the capacitor bank to further facilitate the discharge of capacitors. Different combinations of L and C were used, to emulate the prospective fault current and circuit frequencies. A bistable pneumatic switch was used to discharge the capacitor bank once it had reached the required charging voltage, V_S.

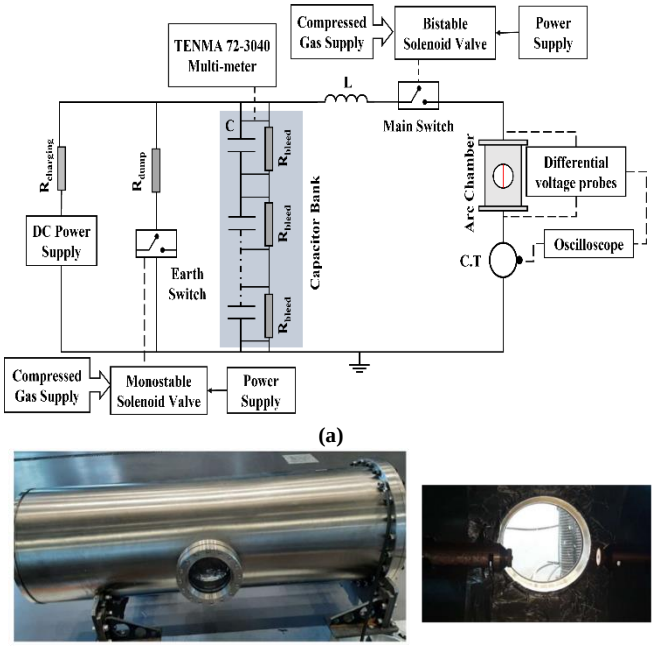

Fig. 1. (a) A schematic diagram of the high current test circuit (b) arc vacuum chamber with the arc electrodes.

Arc initiation was carried out using a fuse wire of 0.2 mm diameter connected between the copper electrodes in a vacuum vessel capable of operating at a range of pressures (Fig. 1(b)). Fuse wires were used to recreate the arc initiation [20] to avoid incorporating an AC triggering source or develop complex moving contacts. The arc current and arc voltage were measured using a current transformer (Pearson model 4418, 0.001 V/A) and a differential voltage probe (Cal Test Electronics, CT4079-NA, 15 kV) respectively. The charging

voltage across the capacitors was measured using a TENMA voltage probe and a multi-meter.

The arc behavior due to effects of circuit frequency (0.5 to 2 kHz), arc current (25 to 100% of maximum current), electrode gap (2.5 to 40 mm) and pressure (0.2 to 1 bar) were investigated. In all the tested configurations, to ensure equipment is operated within its ratings, the arc current was calculated to not exceed 5 kA as in

$$I_{peak} \cong \frac{V_s}{2\pi f L} e^{-\frac{R}{8Lf}}. \quad (1)$$

where f is frequency in Hz and R is the estimated circuit resistance in Ω with a V_S of 0.65 kV across each capacitor. Frequencies in the kHz range are chosen to replicate high-speed operations aiming at lower inductance and smaller size generators [21]. Higher voltage systems operating at variable frequencies in the range of 360-800 Hz already exist in Boeing 787. Higher ranges were only tested such as in the E-Fan X demonstrator, which ran at 1500 Hz, before it ended in 2020 [18]. Details of inductor-capacitor combination examples used in this work alongside the tested charging voltages are depicted in Table I.

TABLE I
CAPACITOR AND INDUCTOR COMBINATIONS USED TO PRODUCE DIFFERENT FREQUENCIES.

V_S (kV)	Frequency (kHz)	Capacitance (μF)	Inductance (μH)
3.1	2.0	125.0	50.0
4.2	1.5		90.1
6.3	1.0		202.0
2.1	2.0	187.5	33.8
2.8	1.5		60.0
4.2	1.0		135.1
1.0	2.0	375.0	16.9
1.4	1.5		30.0
2.1	1.0		67.5

A stainless streel pressure vessel, rated up to 10 bar and with a volume of ~158 liters, was used to investigate the arc behavior under pressures of 1, 0.6 and 0.2 bar, which corresponds to conditions expected in a non-pressurized aircraft compartments at ground level, approximately 15,000 feet, as experienced by vertical take-offs/landings in flying taxis, and approximately 40,000 feet, which is the typical cruise altitude of commercial aircrafts, respectively. The vessel was fitted with a support plate for the fuse wire with a variable gap between the two electrodes. For low pressure tests, the vessel pressure was reduced to 0.2 and 0.6 bar via a vacuum compressor. Pressure was regularly checked using a plug-in digital gauge to ensure no change in pressure. All pressure values indicated in the present work are in absolute. An identical procedure was repeated after each arc ignition.

B. Data Processing

Current and voltage signals were recorded for arcs in underdamped circuits of decaying fault current magnitudes up to 4.6 kA and frequencies from 0.5 to 2 kHz. The arcs generated in this testing are self-extinguishing and behave as a non-linear resistive circuit element, which changes as a function of the injected current and the electrode gap. The arc duration is defined by the energy stored in the capacitor bank and the level of damping resulting from the resistance of the arc. While these circuits see a decrease in current every half cycle, it is important to note that this effect would likely not be seen in an aerospace electrical system where a more constant level of fault current is expected. Arcs were analyzed based on the current and voltage waveforms by calculating the associated arc resistance, conductance, power injected into the arc and arc energy. The arc energy was calculated using the instantaneous integral of the arc power. For all experiments, unless otherwise stated, only the first half cycle was analyzed as it represents a realistic approximation of a practical AC system in which a constant value of arc current may flow. The analyzed data were processed using median filtering to reduce undesired noise whilst preserving the required waveform properties.

III. RESULTS AND DISCUSSION

A. Effect of Electrode Gap

Figs. 2(a) and 2(b) show the effect of varying electrode gap on voltage and current characteristics for a 4.6 kA arc in a 1.5 kHz circuit. While the electrode gap does not equate to the actual arc length, it infers a minimum value of arc length and is likely to be a close approximation to the arc length in the first half cycle before the arc elongates further. As expected, the electric arc behaves as a non-linear resistive element. Fig. 2(a) shows an increase in arc voltage as the electrode gap is widened. The voltage increases, sub-linearly, by a factor of four when the electrode gap was increased from 2.5 to 40 mm due to the higher voltage drop across the longer arc column (assuming every arc has a constant cross-section). The average arc voltage is also changing and does not maintain a constant value due to the stochastic changes of the arc which involve changing length and temperature. At current zero, an arc voltage overshoot is sometimes observed, e.g., at 2 ms for 10 mm, which represents the sudden increase in arc resistance as the current reaches the zero crossing. The electrode voltage drop, $V_{electrode}$, was estimated to be between 14.97 to 33 V for 4.6 kA arcs in the range of 1 to 2 kHz where for shorter gaps $V_{electrode}$ is not negligible. In [22], $V_{electrode}$ was reported to be 16.3 V irrespective of current magnitude or frequency whilst in [23] it was shown to be in the range of 20 to 40 V regardless of the gap length. It can be seen in Fig. 2(b) that the arc current recorded a small decrease of 4% within the first half cycle when the electrode gap was increased from 2.5 to 40 mm with a lower arc duration. The current flowing into the circuit, 4.6 kA, when compared with the value expected from theory, 4.75 kA, has a higher degree of damping as a result of the arc resistance. However, both waveforms remain a damped sinusoid with no change at current-zero. This is due to the arc presenting a higher resistance to the test circuit and thereby resulting in an increased rate of damping. It illustrates the challenge in delivering a high-current test circuit at higher frequencies for use in qualification tests of future aircraft electrical systems. The stored energy in capacitors must be considerably high if capacitor banks are used

to support testing.

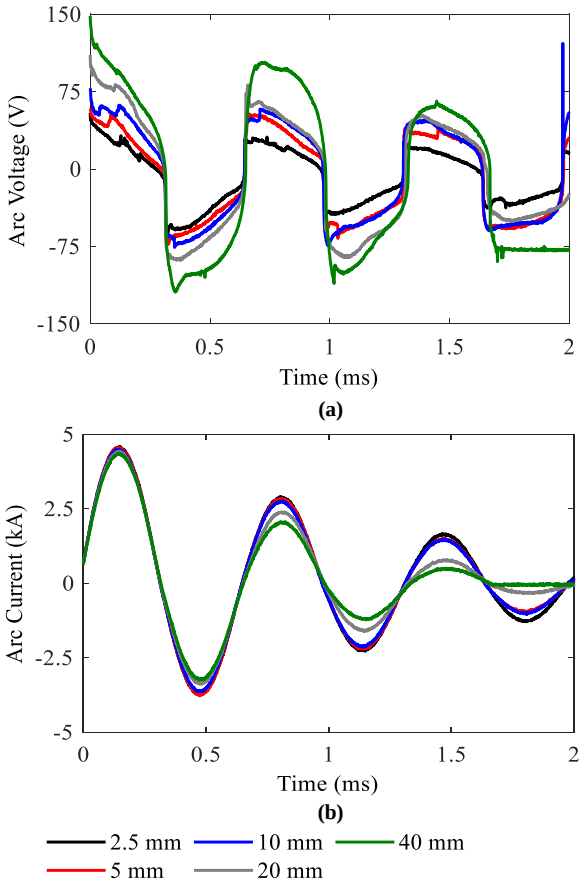

Fig. 2. The variation in (a) arc voltage and (b) arc current of a 4.6 kA arc across electrodes gaps of 2.5 to 40 mm in a 1.5 kHz circuit under atmospheric pressure.

B. Effects of Circuit Frequency and Pressure

This section investigates the change in the arc characteristics as a function of the circuit frequency, tested for pressures of 0.2 and 1 bar and a fixed electrode gap of 2.5 mm. The test frequencies were achieved by varying the inductance and capacitance values whilst maintaining an arc current of 2.4 and 4.6 kA. The values of the capacitors bank and the coil-formed inductance used to produce the required frequencies are depicted in Table II.

Fig. 3 shows the effect of varying circuit frequency on the arc voltage waveform. The ambient pressure was also investigated to determine whether the change in frequency could cause an adverse effect in a low-pressure environment. From experiments, as the circuit frequency increases, the arc exhibits two main changes: (i) a slight decrease in the arc voltage amplitude and (ii) a higher rate of change in voltage, *dV/dt*. The arc voltage slightly reduces for higher frequencies due to the lower inductance value in the test circuit being used, which introduces less damping and lower circuit resistance (Table II). As the pressure is reduced to 0.2 bar, there is a reduction in the arc voltage magnitude. This is due to the low mean electric field of the arc column at low pressure which increases the electrical conductivity for arc temperatures from 5,000 to 12,000 K [8]. At higher frequencies, the arc voltage difference between 0.2 and 1 bar reduces as observed between Figs. 3(a) and 3(c) for 1.5 and 0.5 kHz arcs, respectively. The waveform slopes in Fig. 3 represents *dV/dt*, which reduces with lower frequencies for both 0.2 and 1 bar. The difference in arc voltage remains unclear but may be due to the burning of fuse wire. The arc voltage magnitude, circuit arrangement and parameters contribute to the nonlinearity of the arc voltage waveform seen in Fig. 3. Their combined effect disrupts the arc voltage curve and contributes to adding high harmonics to the signal [24].

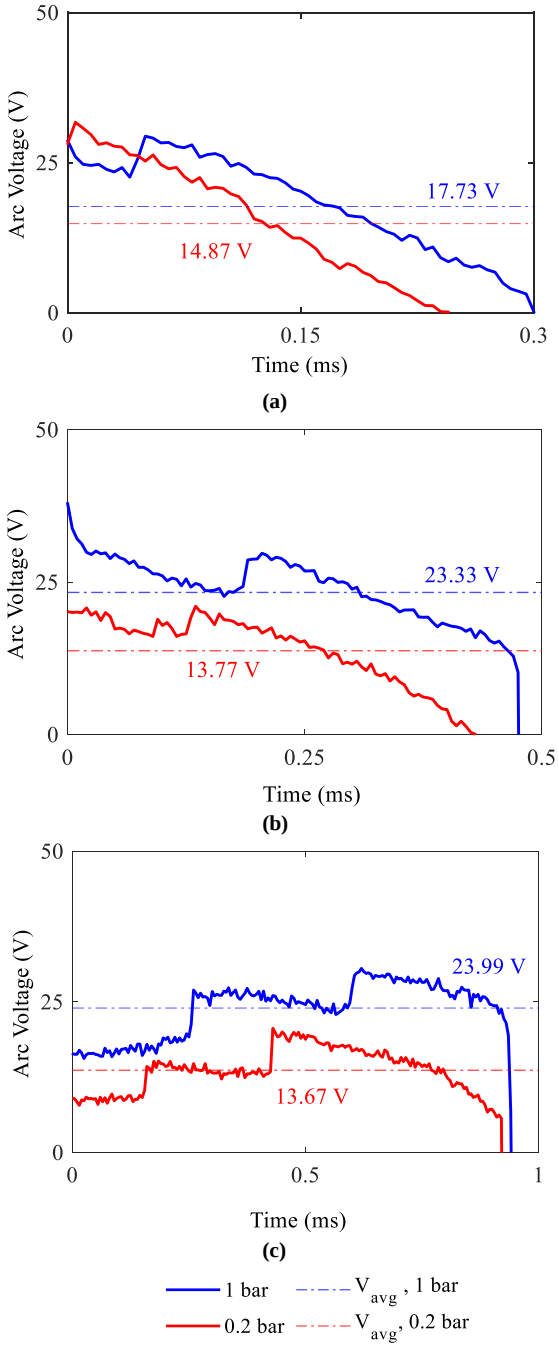

Fig. 3. The arc voltage at circuit frequency of (a) 1.5 kHz, (b) 1 kHz, and (c) 0.5 kHz with 2.4 kA current peak tested for a 2.5 mm electrode gap and under pressures of 0.2 and 1 bar (dashed lines: average arc voltage calculated based on the first half cycle).

TABLE II
CAPACITOR AND INDUCTOR COMBINATIONS USED TO INVESTIGATE THE FREQUENCY EFFECT.

Current (kA)	Frequency (kHz)	Inductance (μH)	Capacitance (μF)
2.4	0.5	270.2	375.0
	1.0	135.1	187.5
	1.5	90.1	125.0
4.6	1.0	67.5	375.0
	2.0	33.8	187.5

Fig. 4 shows the arc voltage gradient of a 4.6 kA arc. For shorter electrode gaps, the channel resistance is lower, and the total arc voltage is dominated by the anode and cathode volt drops. This leads to a high-voltage gradient to maintain the arc across the electrode gap. As the electrode gap increases, the arc voltage gradient reduces and the arc voltage almost entirely falls across the arc channel leading to a relatively constant arc voltage and a less distorted square wave observed for longer electrode gaps (i.e., >40 mm in this study). This means that the relationship between the arc voltage and arc length can be approximated as directly proportional with longer electrode gaps, whilst it cannot be presented by a simple scalar for shorter electrode gaps. Unlike power system equipment such as the 15 kV switchgear and medium-voltage motor control, MCC, the compact designs of aircrafts, suggest that arc faults will be for shorter gap spacing between adjacent electrical systems. This makes the estimation of arc voltage for aircraft faults difficult due to the non-linear relationship between arc voltage and arc length at shorter electrode gaps. For results obtained at 0.2 bar pressure, the voltage gradient is generally lower than their counterparts at 1 bar regardless of the circuit frequency, as shown in Fig. 4. This may be a direct consequence of arc elongation at lower pressure.

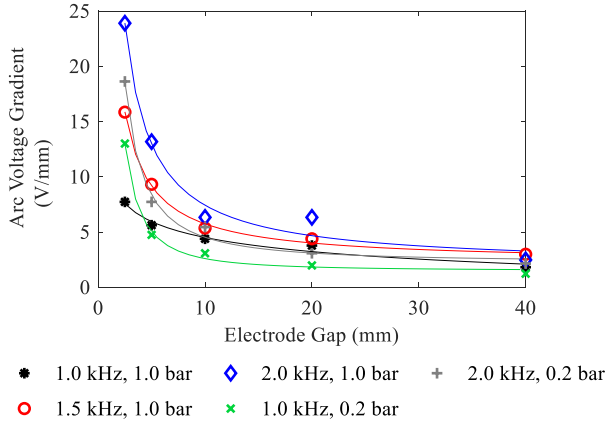

Fig. 4 The arc voltage gradient of a 4.6 kA arc as a function of electrode gaps for 1, 1.5 and 2 kHz (marker: experimental data; solid line: fitting curves).

C. V-I Characteristics of Electric Arcs

This section explores the V-I characteristics of arcs under pressures of 0.2 and 1 bar and across electrode gaps of 2.5 and 40 mm. Fig. 5 shows the flow of the first two cycles of a 4.6 arc which form two hysteresis loops. Each loop in Fig. 5(a) illustrates the arc in terms of voltage-current relationship and the area of the loop. At every first cycle, before the arc is completely established, a noisy higher arc voltage peak is sometimes seen at arc initiation. The presence of fuse wire to ignite the arc and its vaporization could be responsible for this event as the wire burning changes the surrounding dynamic for the first few microseconds. For fuse wires stretched across electrode gaps, a high current density is required to vaporize the fuse wire. The rise in arc voltage corresponds to the sudden application of voltage leading to wire vaporization across the electrode gap. At this stage, the current starts to flow through the wire and subsequently through the arc with an upsurge due to the high current density and the arc voltage drops. As the current continues to increase, the arc voltage remains at a relatively constant value and independent of the arc current. Prior to arc extinguishing, the arc voltage starts to increase slowly and until I_{arc} is zero. At current zero, arc resistance, as opposed to arc conductance, is momentarily at a high value and results in a significant voltage drop across the electrode gap. The electrode gap is almost immediately under voltage stress and the current begins to flow in the opposite direction. Other cycles exhibit similar behavior but with a higher energy dissipation as the arc becomes cooler.

Figs. 5(b) shows the V-I characteristics of the same arc under low pressure. The loop area represents the integral of the product of voltage and current (i.e., arc power). Arcs under atmospheric pressure, Fig. 5(a), have larger loops which corresponds to the slightly higher arc voltage leading to higher arc energy. A typical V-I hysteresis loop would have two matching half cycles. In this case, the changes associated with the arc voltage, arc current, and the circuit damping resulted in the loop having a different shape every half cycle. A small reduction in the arc voltage can sometime be observed as the arc progresses towards the peak current. This is normally counteracted by a voltage increase to maintain the arc as illustrated in Fig. 5(a) for the 2.5 mm electrode gap during the first cycle (i.e., t= 1 ms).

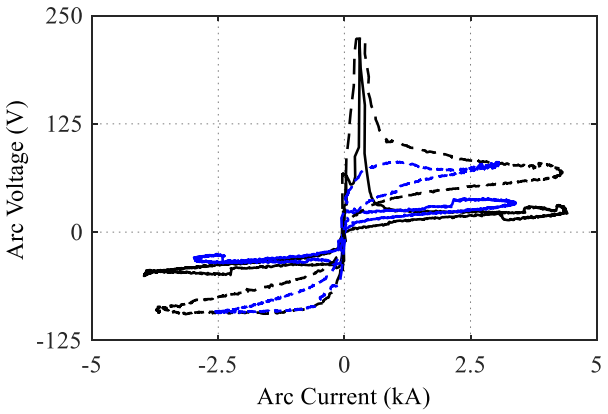

(a)

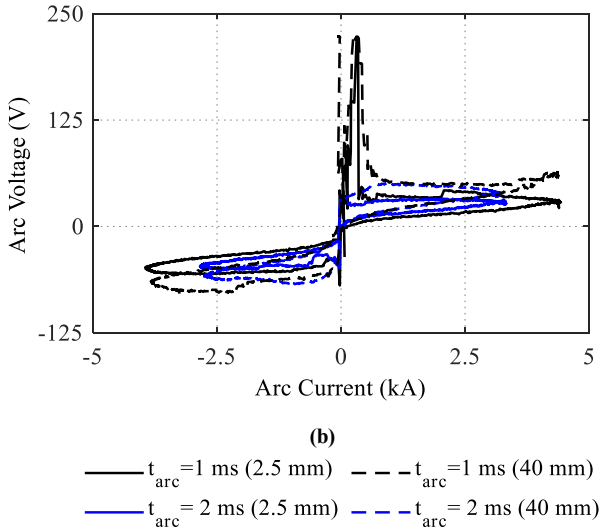

Fig. 5 V-I characteristics of the first two cycles of 4.6 kA arcs in a 1 kHz circuit for 2.5 and 40 mm electrode gaps at (a) 1 and (b) 0.2 bar (clockwise change).

D. Arc Energy Calculations

Sections 3.1 to 3.3 explored a range of parameters that impact arc behavior in future higher voltage aerospace electrical systems, which in return affect the accumulative arc energy. This section presents the arc energy calculations associated with different arcs. The arc energy is an important parameter in evaluating the hazards associated with arc faults. It results in erosion of metallic electrodes; significant levels of heat transfer and pressure increase that all constitute potential hazards to nearby systems / structures or personnel. In [25], it was mentioned that over 50% of the arc energy is responsible for melting and vaporizing metal and insulation, whilst the remaining arc energy is transferred to the arc column contributing to the processes of conduction, convection, or radiation. The accumulative arc energy of a 4.6 kA peak arc current during the first cycle at atmospheric pressure is shown in Fig. 6. During (A), the arc energy is relatively low, and the arc is not yet sustained. As the current increases, the energy supplied to the arc increases and the arc temperature is at its highest corresponding to the peak current (B). Hence, the majority of arc energy transfer occurs during the middle of half cycles. The rise of energy during these time durations contribute to pressure changes within the vessel. For this test, the vessel volume is sufficiently large, so the pressure change is negligible. The energy continues to accumulate and momentarily saturates at (C) where the current passing through the arc channel is zero. The arc energy will continue to increase until the end of the half cycle as shown in Fig. 6.

Fig. 7 illustrates the energy variation during the entire duration of the arc at different pressures. The arc voltage at lower pressures (i.e., 0.2 bar) reduces resulting in a lower arc energy, which does not reflect the worst-case scenario. The arc at 1 bar produces a higher magnitude of arc energy than the arcs at 0.6 and 0.2 bar. Similar results were observed in the repeated experiments. While our work showed that a reduction in pressure reduces arc voltage per length, the work in [8] showed that arc elongation could then result in an overall higher arc energy.

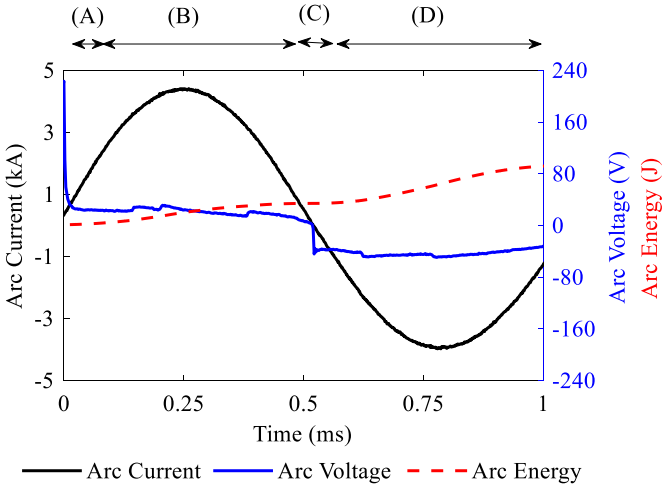

Fig. 6 The variation of arc energy as an AC arc current sustains a 4.6 kA arc at 1 bar in a 1 kHz circuit across an electrode gap of 2.5 mm.

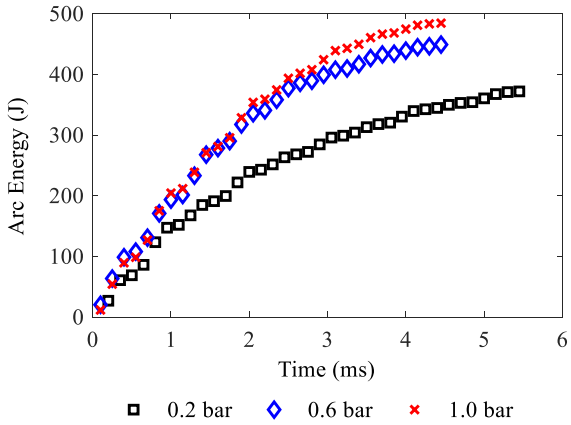

Fig. 7 Arc energy accumulation for a 4.6 kA arc across an electrode gap of 2.5 mm, tested for pressures of 0.2, 0.6 and 1 bar.

IV. Arc Modeling: Model Development and Results

A. Model Theory: Hypothesis and Equations

In Section 3, it was shown that high current and high frequency arcs behave as non-linear resistive elements in which the arc resistance is directly affected by circuit parameters. This behavior can be explained by a set of time-varying differential equations where the arc conductance varies as a function of arc current, voltage, and other arc parameters. There is limited literature published on modeling of high frequency and high current arcs. This is somewhat expected as the current maximum operating frequency is 400-800 Hz for application in more-electric aircraft and high current arcs at 50/60 Hz are widely investigated for circuit breaker applications. The underlying challenge with modeling of future higher voltage aerospace electrical systems is the lack of knowledge on the relationship between the arc voltage with parameters such as frequency, pressure, and electrode gap. Figs. 6 and 7 in Section 3 showed that the arc energy increases non-linearly with the electrode gap. Unlike longer gaps, short arcs cannot be simply represented by Equation (2) as the arc voltage drop at the electrode cannot be neglected. Based on the experimentally obtained results, for electrode gaps between 2.5 to 100 mm, the arc energy increase can be represented by a natural logarithmic

equation. Hence, the effect of arc elongation in an AC arc can be incorporated by scaling the arc model equation with the correct arc length function.

$$U_{arc} = BL \tag{2}$$

where B is the arc voltage gradient and L is arc length.

B. New Model Development and Implementation: Based on a Modified Mayr Model

The instantaneous arc conductance for AC arcs can be calculated by the arc current and voltage at a given time. According to [26] the arc conductance can be calculated using the Mayr-based Equation (3) with two parameters: time constant, τ and cooling power, P_{out}. The cooling power constant depends on two fitting parameters, C_1 and P_o defined in Equation (4). Both fitting values along with the arc time constant can be estimated as reported in [26].

$$\frac{1}{g}\frac{dg}{dt} = \frac{1}{\tau}\left(\frac{ui}{P_{out}(i)} - 1\right) \tag{3}$$

$$P_{out}(i) = p\,(P_0 + C_1 i) \tag{4}$$

where u is the arc voltage, i is the arc current, τ is the time constant, p is the gas pressure, C_1 and P_o are the fitting parameters.

In Section 4.1, it was explained that the arc energy varies non-linearly with the electrode gap, which can be represented by a natural logarithmic function. To incorporate the arc length effect into the model, the cooling power constant is scaled by the natural logarithmic function of the electrode gap (Equation 5). The arc model was integrated in the circuit shown in Fig. 1 using Simulink to replicate similar arc discharge testing setup. In this model, it is assumed that the arc length is equal to the electrode gap. Although this assumption is not reflective of the physical nature of a high current short duration arc, given their capability of varying drastically from the electrode gap, it still gives good estimation of the arc voltage for the tested conditions. P_0 and C_1 are estimated from the comparison of the simulated and experimental arc voltage waveforms to calculate the lowest RMS value as the worst-case scenario. Both parameters, P_0 and C_1, are then multiplied by the logarithmic relationship between the arc energy and arc length.

$$P_{out}(i) = (P_0 + C_1 i)\,ln\,l \tag{5}$$

where P_{out} is the cooling power in W, i is the arc current in A, l is the electrode gap in mm, P_o and C_1 are model parameters.

Fig. 8 compares the arc model waveforms to the experimental results for a 4.6 kA in a 1 kHz circuit as a function of two electrode gaps: 5 and 100 mm under atmospheric pressure. A peak is observed during the first microseconds due to the action of the fuse wire, which is resembled by the model by virtue of the initial arc conductance, g(0). Those peaks are present at each current-zero crossing to model the high resistance when the current is in a low region. In the high current regions, for the 2.5 to 100 mm range, the modeled waveforms yield good agreement with the experimental results for up to 100 mm. Model results deviates from experimental at current-zero and near the current-zero crossing as the interruption region is not considered in this model.

Table III shows the model and experimental results for a 4.6 kA at 1 kHz under 1, 0.6 and 0.2 bar. Based on Equation (5), the modified model is in good agreement with the experimental results for 1 bar (Fig. 8). As the pressure reduces, satisfactory results are observed for 2.5 mm. At 40 mm, a significant difference is seen between the results of the modeled arc (Equation (5)) and the experimental data. This is because Equation 5 does not account for pressure variation and only assumes the arc voltage change is directly associated with the logarithmic function of the electrode gap.

Equation (6), a modified version of Equation (5), estimates the cooling power as a function of the electrode gap and air pressure which then feeds into the estimation of arc voltage. This modification improves the applicability of the new arc model to include arc simulations at aeronautical conditions. Simulation results and comparisons of Equation (5) and Equations 6 are shown in Fig. 9. It illustrates good agreement with the experimental data where the reduction in pressure reduces the cooling power leading to a slow exponential reduction in the average arc voltage across the electrode gap.

$$P_{out}(i) = \left(P_0 + \frac{C_1}{e^{0.5(1-p)}} i\right) ln\,l \tag{6}$$

where p is air pressure in bar absolute and P_0 and C_1 are equal to 10^{-4} W·mm^{-1} and 20 W·bar·A^{-1}·mm^{-1}, respectively.

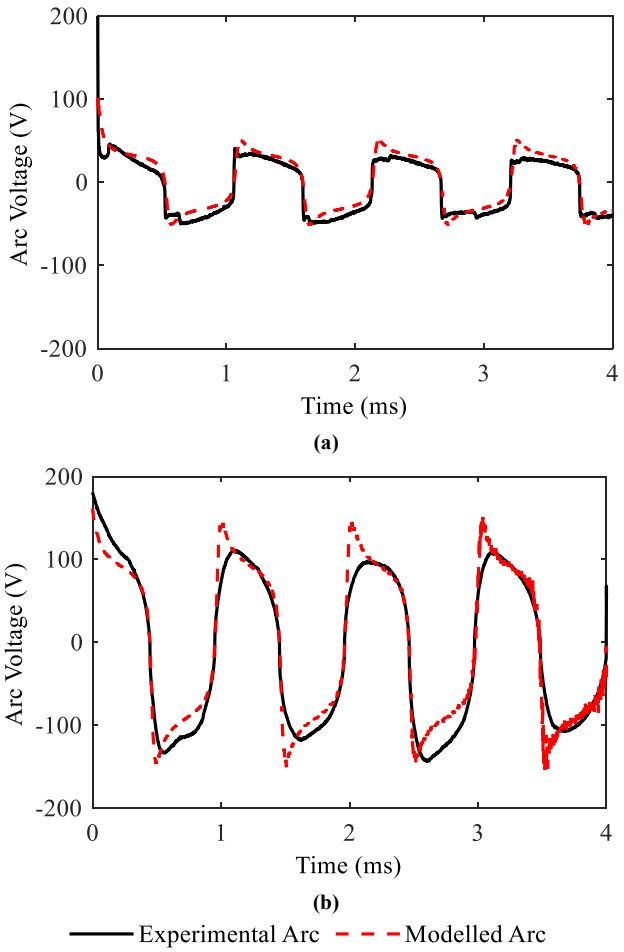

Fig. 8 Time-varying simulated arc voltage of a 4.6 kA arc across (a) 5 and (b) 100 mm.

TABLE III
A COMPARISON OF THE EXPERIMENTAL ARC VOLTAGE VALUES AND THE MODEL RESULTS FOR 2.5 AND 40 MM UNDER 1, 0.6 AND 0.2 BAR ABS.

Electrode gap	2.5 mm			40 mm		
Pressure (bar)	$V_{Experimental}$	Equation (5)	Equation (6)	$V_{Experimental}$	Equation (5)	Equation (6)
1	21.22 V	19.52 V	19.52 V	67.40 V	78.99 V	78.99 V
0.6	17.29 V	20.64 V	16.90 V	64.98 V	77.31 V	63.30 V
0.2	14.89 V	18.47 V	12.21 V	45.02 V	73.18 V	40.05 V

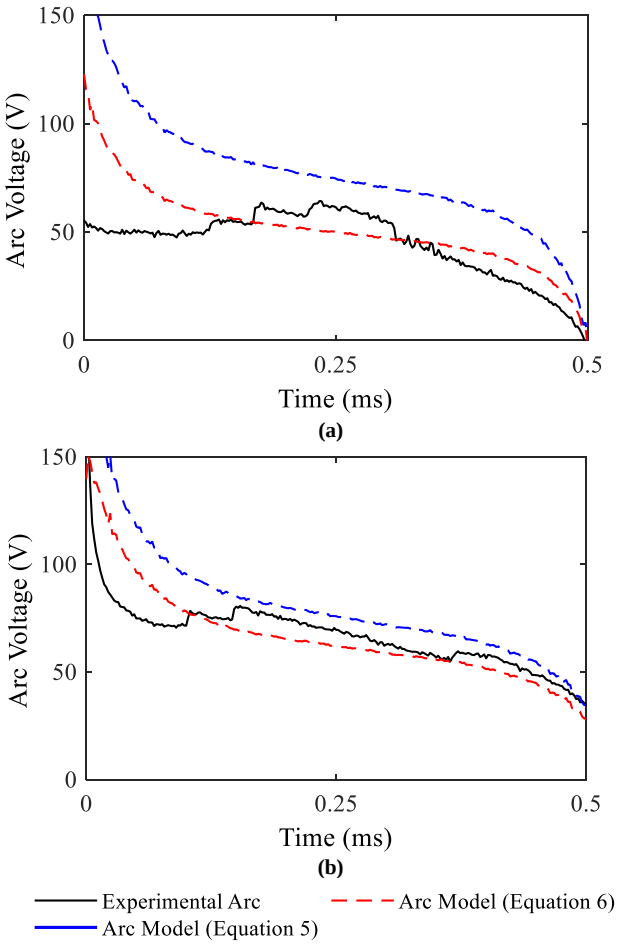

Fig. 9 Time-varying simulated arc voltage waveforms of a 4.6 kA arc under 1 kHz for (a) 0.2 and (b) 0.6 bar, tested for a 40 mm electrode gap.

C. Model Applicability Validation

The modified arc model was compared with experimental and modeling work on AC arcs in air under atmospheric pressure from previous research at a range of applications including power and high frequency, high current, and high voltage. The results, which validate the applicability of our model to a wide range of applications, are shown below:

1) **High Current, Low Voltage, Power Frequency**
According to Wu et al. [27], low voltage AC arcs of short durations can be modeled as shown in Equation (7). This model was proven applicable for single phase arc currents in the range of 3 to 100 kA. According to Equation (7), for an electrode gap of 60 mm at a rated voltage of 50 V, the estimated arc voltage is 82.28 V. By incorporating our model, Equation (6), in a representative AC system on Simulink, an average arc voltage of 81.82 V is obtained. For a 100 mm electrode gap, Equation (7) yields 75.58 V, which contradicts the increase in arc voltage as a response to longer electrode gaps. On the other hand, our model yields 92.34 V which is representative of the expected arc voltage.

$$U_{arc} = \begin{cases} 53.4 + 0.018U_n^{0.84}d & d \le 60\ mm \\ 2.355U_n^{0.74} + 0.33d & d > 60\ mm \end{cases} \quad (7)$$

where U_n is rated voltage in V, and d is the electrode gap in mm.

2) **High Current, High Voltage, Power Frequency**
A Cassie based arc model in [28], models electrical arc with respect to the change in the arc diameter, Equation (8). It correlates the change in arc diameter to the magnitude of arc current, where the model covers low and high current regions. The free burning arc was tested for 1.5 kA, 10 mm electrode gap and power frequency. Measured and simulated arc voltages were compared with other conventional models viz. KEMA, Schwarz and Schwamaker. At the first half period, the arc voltage is estimated at 53 V compared with 46.2 V using Equation (6).

3) **Low Current, High Voltage, High Frequency**
Methods of parameter determination and arc characteristics description were reviewed by Walter and Franck in [29]. Free burning frequencies in the range of 0.5 to 16 kHz were the main interest of this research. The two Mayr parameters P_{out} and τ were estimated using four different methods: iterative indirect method, direct parameter separation method, direct multiple gradient method, and staircase method. The later has shown that for 850 Hz, an average arc voltage is estimated at 43.94 V with no significant difference for 3.6 and 8.3 kHz. Equation (6) has shown a satisfactory estimate of 32.36 V.

V. CONCLUSION

A high-frequency test setup was developed to investigate the behavior of AC arcs in a pressure vessel. The underdamped test circuit assessed the arc performance characteristics under aeronautical conditions for arc currents up to 5 kA, frequencies in the range of 0.5 to 2 kHz and electrode gaps between 2.5 to

40 mm under pressures of 0.2, 0.6 and 1 bar. The main conclusions of this work are as follows:

1) **Generalized modeling approach without recourse to experiment –** arc current and arc voltage waveforms obtained at 1, 0.6 and 0.2 bar were analyzed and fed into an arc model that defines the relationship between the electrode gap and the arc cooling power through a natural logarithmic function. Good agreement between experimental and simulated results is achieved for electrode gaps up to 100 mm and frequencies between 1 to 2 kHz. The initial modified model showed deviation at longer gaps and lower pressures. A further improved model was developed that was able to correlate the change in pressure to the arc cooling power. This generalized modeling approach can be used to predict energy levels for a given fault current and fault duration, which could eliminate the need to develop complex experimental setups to reproduce arc faults under challenging conditions.
2) **Testing methodology for arc hazards under aeronautical conditions –** pressure variability, setup versatility and high-power generation are three important of aspects of the designed setup. Tests carried out at atmospheric pressure represent the worst-case scenario for arc duration up to 11 ms. For arcs tested under 1, 0.6 and 0.2 bar, atmospheric arcs produced the highest energy. Representative tests under a low-pressure environment may be unnecessary for the specified test conditions to assess arc hazards. The setup is applicable for tests of other applications including at power frequency and higher voltages.
3) **Electrical characterization of high frequency and high current arcs –** the analysis of the arc voltage and current waveforms showed that higher frequency arcs display a slightly lower average arc voltage due to the lower inductance used to produce the frequency. Consequently, lower arc energy is produced due to corresponding changes in the circuit impedance of the test setup. The effect of higher frequencies on the voltage gradient is minimal for longer electrode gaps. In general, lower voltage gradients were captured for tests undertaken at lower frequencies. Arc energy is found to be higher with longer gaps but not necessarily higher per unit length due to the potential arc elongation that could occur at lower pressures.

REFERENCES

[1] *European Aviation Environmental Report 2019*. Publications Office of the EU, 2019.
[2] J. Domone, "The challenges and benefits of the electrification of aircraft," 2018.
[3] B. Brusso, "History of Aircraft Wiring Arc-Fault Protection," *IEEE Industry Applications Magazine*, pp. 6–11, 2017.
[4] "INSIGHT_07-Electrical Power Systems," Cranfield, 2018.
[5] B. Sarlioglu and C. T. Morris, "More Electric Aircraft: Review, Challenges, and Opportunities for Commercial Transport Aircraft," *IEEE Trans. Transp. Electrif.*, vol. 1, no. 1, pp. 54–64, 2015.
[6] K. Keller, "Understanding Arc Flash and Arc Blast Hazards," in *Electrical Safety Code Manual: Plain Language Guide to National Electrical Code, OSHA and NFPA 70E,* Oxford: Elsevier, 2010, pp. 143–170.
[7] G. Belijar, G. Chanaud, L. Hermette, and A. Risacher, "Study of electric arc ignition, behavior and extinction in aeronautical environment, in presence of FOD," *HAL*, vol. hal-016561, pp. 1–8, 2017.
[8] R. Landfried, L. Savi, T. Leblanc, and P. Teste, "Parametric study of electric arcs in aeronautical condition of pressure," *Eur. Phys. J. Appl. Phys.*, vol. 67, no. 2, pp. 1–7, 2014.
[9] R. Landfried, M. Boukhlifa, T. Leblanc, P. Teste, and J. Andrea, "Stability, spatial extension and extinction of an electric arc in aeronautical conditions of pressure under 540 V DC," *Eur. Phys. J. Appl. Phys.*, vol. 87, no. 3, pp. 1–9, 2019.
[10] M. Boukhlifa, J. Andrea, T. Klonowski, R. Landfried, and P. Teste, "The Impact of Pressure on Electric Arcs Switch-off," *2019 IEEE Holm Conf. Electr. Contacts*, 2019.
[11] H. El Bayda, F. Valensi, M. Masquere, and A. Gleizes, "Energy Losses from an Arc Tracking in Aeronautic Cables in DC Circuits," *IEEE Trans. Dielectr. Electr. Insul.*, vol. 20, no. 1, pp. 19–27, 2013.
[12] K. Zeng, L. Xing, Y. Zhang, and L. Wang, "Characteristics analysis of AC arc fault in time and frequency domain," *2017 Progn. Syst. Heal. Manag. Conf.*, 2017.
[13] J. Yuan, W. Jianwen, and J. Bowen, "Reignition after Interruption of Intermediate-Frequency Vacuum Arc in Aircraft Power System," *IEEE Access*, vol. 6, pp. 8649–8656, 2018.
[14] M. Borghei and M. Ghassemi, "Insulation Materials and Systems for More and All-Electric Aircraft: A Review Identifying Challenges and Future Research Needs," *IEEE Trans. Transp. Electrif.*, vol. 7, no. 3, pp. 1930–1953, 2021.
[15] J. Jiang *et al.*, "Optical sensing of partial discharge in more electric aircraft," *IEEE Sens. J.*, vol. 20, no. 21, pp. 12723–12731, 2020.
[16] T. André, F. Valensi, P. Teulet, Y. Cressault, T. Zink, and R. Caussé, "Arc tracking energy balance for copper and aluminum aeronautic cables," *J. Phys. Conf. Ser.*, vol. 825, pp. 1–10, 2017.
[17] M. Borghei and M. Ghassemi, "Insulation Materials and Systems for More and All-Electric Aircraft: A Review Identifying Challenges and Future Research Needs," *IEEE Trans. Transp. Electrif.*, 2021.
[18] "Airbus and RollsRoyce end E-Fan X hybrid-electric aircraft initiative," *Green Car Congress*, 2020. https://www.greencarcongress.com/2020/05/20200501-airbus.html (accessed Oct. 21, 2022).
[19] "Aircraft Electrical Voltage Level Definitions AIR7502," 2021.
[20] H. El Bayda, F. Valensi, M. Masquere, and A. Gleizes, "Energy losses from an arc tracking in aeronautic cables in DC circuits," *IEEE Trans. Dielectr. Electr. Insul.*, vol. 20, no. 1, pp. 19–27, 2013.
[21] J. K. Noland, M. Leandro, J. A. Suul, and M. Molinas, "High-Power Machines and Starter-Generator Topologies for More Electric Aircraft: A Technology Outlook," *IEEE Access*, vol. 8, pp. 130104–130123, 2020.
[22] Y. Yokomizu, T. Matsumura, R. Henmi, and Y. Kito, "Total voltage drops in electrode fall regions of SF6, argon and air arcs in current range from 10 to 20 000 A," *J. Phys. D. Appl. Phys.*, vol. 29, no. 5, pp. 1260–1267, 1996.
[23] A. P. Strom, "Long 60-Cycle Arcs in Air," *Trans. Am. Inst. Electr. Eng.*, vol. 65, no. 3, pp. 113–117, 1946.
[24] V. Terzija, G. Preston, M. Popov, and N. Terzija, "New static airarc EMTP model of long arc in free air," *IEEE Trans. Power Deliv.*, vol. 26, no. 3, pp. 1344–1353, 2011.
[25] J. R. Riba, Á. Gómez-Pau, M. Moreno-Eguilaz, and S. Bogarra, "Arc tracking control in insulation systems for aeronautic applications: Challenges, opportunities, and research needs," *Sensors*, vol. 20, no. 6, pp. 1–16, 2020.
[26] L. van der Sluis, W. R. Rutgers, and C. G. A. Koreman, "A physical ARC model for the simulation of current zero behavior of high-voltage circuit breakers," *IEEE Trans. Power Deliv.*, vol. 7, no. 2, pp. 1016–1022, 1992.
[27] H. Wu, X. Li, D. Stade, and H. Schau, "Arc fault model for low-voltage AC systems," *IEEE Trans. Power Deliv.*, vol. 20, no. 2, pp. 1204–1205, 2005.
[28] A. Khakpour, S. Franke, S. Gortschakow, D. Uhrlandt, R. Methling, and K. D. Weltmann, "An Improved Arc Model Based on the Arc Diameter," *IEEE Trans. Power Deliv.*, vol. 31, no. 3, pp. 1335–1341, 2016.
[29] M. Walter and C. Franck, "Improved method for direct black-box arc parameter determination and model validation," *IEEE Trans. Power Deliv.*, vol. 29, no. 4, pp. 580–588, 2014.

Abir Alabani (Student Member, IEEE) obtained a first-class BEng (Hons) degree in Electrical and Electronic Engineering in 2018 from the University of Manchester. She is currently undertaking a Ph.D. degree in arc track characterization of high voltage aeronautical systems at the High Voltage Laboratory at The University of Manchester, UK. Her research interests include arcing faults in aeronautical power systems, SF_6 alternatives and gas discharge in HV equipment.

Prem Ranjan (Member, IEEE) obtained the B.Tech. degree in Electrical and Electronics Engineering from NIT Calicut in 2015 and the MS, Ph.D. degrees in Electrical Engineering from IIT Madras, Chennai, India in 2019. He worked as a postdoc researcher at High Voltage Lab, The University of Manchester, UK. Currently, he is working at Deeside Centre for Innovation, National Grid, UK. His research interests include exploding wire and condition monitoring of power apparatus.

Jun Jiang (Senior Member, IEEE) received the B. E. degree in electrical engineering and automation from China Agricultural University (CAU) in 2011 and Ph.D. degree in high voltage and electrical insulation from North China Electric Power University (NCEPU) in 2016. During 2019-2020, he was an academic visitor at the Department of Electrical & Electronic Engineering, School of Engineering, The University of Manchester, UK. He is now working as an Associate Professor in Department of Electric Engineering, Nanjing University of Aeronautics and Astronautics (NUAA), Nanjing, China. His research interests are condition monitoring of power apparatus and optical sensing application.

Lujia Chen (Member, IEEE) obtained a BEng (Hons) degree in Electrical & Electronic Engineering in 2012 and then a PhD in High Voltage Engineering in 2015 from Cardiff University, UK. He is currently Senior Lecturer at The University of Manchester. His research activities are focused on insulating gases with significantly lower environmental impact for high voltage applications.

Ian Cotton (Senior Member, IEEE) received the B.Eng. degree (Hons.) in electrical engineering from the University of Sheffield, Sheffield, U.K. in 1995, and the Ph.D. degree in electrical engineering from The University of Manchester Institute of Technology (UMIST), Manchester, U.K. in 1998. He is currently Professor of High Voltage Technology with The University of Manchester where his research work is based in the high voltage laboratories. He is involved in work relating to power system equipment used in both terrestrial power and transportation systems. He is Technical Director of aerospaceHV Ltd.

Vidyadhar Peesapati (Member, IEEE) received the B.Eng. degree in electrical and electronics engineering, from the University of Madras, Chennai, India, in 2001, and the M.Sc. degree in electrical power systems and the Ph.D. degree in electrical and electronic engineering from The University of Manchester, Manchester, U.K., in 2006 and 2010, respectively. He is currently Senior Lecturer with The University of Manchester, in the area of high voltage systems, asset management, and condition monitoring. He is Charted Engineer (C.Eng.) and a member of the IET.